Nanoscale

Accepted Manuscript

This article can be cited before page numbers have been issued, to do this please use: A. Bertucci, J. Guo, N. Oppmann, A. Glab, F. Ricci, F. Caruso and F. Cavalieri, *Nanoscale*, 2017, DOI: 10.1039/C7NR07814E.

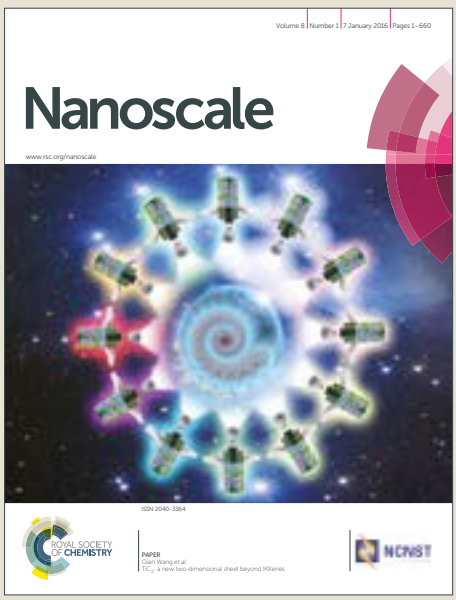

ROYAL SOCIETY OF CHEMISTRY

rsc.li/nanoscale

View Article Online
DOI: 10.1039/C7NR07814E

Journal Name

ARTICLE

Probing Transcription Factor Binding Activity and Downstream Gene Silencing in Living Cells with a DNA Nanoswitch

Received 00th January 20xx,
Accepted 00th January 20xx

DOI: 10.1039/x0xx00000x

www.rsc.org/

Alessandro Bertucci, [ab] Junling Guo, [a] Nicolas Oppmann, [a] Agata Glab, [a] Francesco Ricci, [b] Frank Caruso,* [a] and Francesca Cavalieri* [ab]

Transcription factor DNA binding activity is of pivotal importance in living systems because of its primary involvement in the regulation of genetic machinery. The analysis of transient expression levels of transcription factors in response to a certain cell status is a powerful means for investigating cellular dynamics at the biomolecular level. Herein, a DNA-based molecular switch that enables probing of transcription factor DNA binding activity is directly used in living cells. We demostrate that the DNA nanoswitch allows for dynamic fluorescence imaging of NF-κB and quantification of downstream gene silencing in real time. The present strategy is based on a functional DNA nanodevice that transduces, through a binding-induced conformational change, the recognition of a specific transcription factor into a fluorescent signal. In addition, stochastic optical resolution microscopy, a super-resolution microscopy technique, is used to track the internalization and intracellular trafficking of the DNA nanodevice with high spatial resolution. Overall, it has been shown that a rationally designed DNA nanodevice can be used to achieve rapid, simple, and cost-effective real-time determination of transcription factor binding activity and downstream gene silencing.

Introduction

DNA nanostructures, on account of their programmable nature, can be designed to generate functional materials and devices. DNA nanotechnology has inaugurated a new era of engineering programmable molecular motion with unprecedented control and precision, affording dynamic systems that can process information through finely tuned molecular movements.[1–4] In biological systems, information is processed and signaled through complex pathways governed by dynamic non-covalent interactions. Turning to nature for inspiration, DNA-based bio-actuators can be engineered in such a way to actively interface with biomolecules. This allows for their molecular dynamics to be finely regulated by the interplay with target species in living organisms.[5–9]

One of the most studied intracellular dynamics is the DNA binding activity displayed by transcription factors because of their pivotal role in cellular metabolism and their involvement in processes such as inflammatory response and cancer progression.[10] Therefore, the development of nanodevices for probing of transcription factor (TF) expression, localization, and shuttling is expected to advance molecular biology and diagnostics. This would improve our ability to elucidate TF functions in healthy or diseased states and boost refinement of bio-analytical methods and drug screening assays. As each TF virtually recognizes only a characteristic DNA domain,[11] the idea has naturally emerged that biomimetic DNA nanodevices may be designed to transduce a TF-binding event into a detectable output to support test-tube probing of TF concentration and functional activity. Heyduk and co-workers pioneered the development of fluorescence proximity assays harnessing binding-induced association of DNA recognition fragments.[12] The detection of TFs in solution has subsequently been achieved by employing different techniques.[13–17] Recently, the development of molecular DNA nanoswitches for the quantitative detection of TFs was reported.[18] These DNA nanodevices were conceived as an analytical tool to quantify TF binding activity and concentration in test tubes. They featured a double stem-loop structure that switches from a fluorescent "off-state" to an "on-state" upon binding to the target TF. However, these DNA nanoswitches have never been applied in a complex and dynamic environment such as a living cell. To our knowledge, there are no reports of DNA-based probes employed for the

[a] ARC Centre of Excellence in Convergent Bio-Nano Science and Technology, and the Department of Chemical and Biomolecular Engineering, The University of Melbourne, Parkville, Victoria 3010, Australia E-mail francesca.cavalieri@unimelb.edu.au; fcaruso@unimelb.edu.au
[b] Department of Chemistry, University of Rome Tor Vergata, 00133 Rome, Italy
† Footnotes relating to the title and/or authors should appear here.
Electronic Supplementary Information (ESI) available: [details of any supplementary information available should be included here]. See DOI: 10.1039/x0xx00000x

View Article Online
DOI: 10.1039/C7NR07814E

intracellular monitoring of TF binding activity in living cells. Currently, probing TF levels in vitro or in vivo relies on either the multi-step and reagent-intensive antibody-based staining of fixed cells, or the expression of fluorescent fusion protein tags,[19] or the use of transgenic mice encoding reporter genes under the control of a target TF.[20]

Herein, we demonstrate that a DNA-based molecular switch can bind to a target TF directly in living cells, probing its activity in situ. We show that we can monitor in real -time intracellular expression and localization of NF-κB, translating a TF-responsive DNA nanodevice from test tube to the complex intracellular environment. Importantly, the DNA nanoswitch also serves as a dynamic probe for sensing and comparatively quantifying in real time the intracellular silencing of NF-κB, with no need for reporter genes. This TF-responsive nanoswitch can be potentially used as a simple, rapid, functional sensing device as an alternative to standard antibody-based staining techniques (based on a static structural matching in fixed cells) and multi-step and reagent-intensive reporter gene technologies.

Experimental

Materials

HPLC-purified oligonucleotide DNA sequences modified with either the pair Quasar® 670 (5'-modification)–Black Hole Quencher (BHQ2, internal modification) (NF-κB-switch and Control Sequence) or the pair Quasar® 570 (5'-modification)–Quasar® 670 (internal modification) (STORM beacon) were supplied by Biosearch Technologies (Novato, CA, USA). Non-modified DNA oligonucleotides were purchased from GeneWorks (Thebarton, Australia). PC3 human prostate epithelial cancer cells (CRL-1435) were obtained from ATCC®. Human recombinant NF-κB p50 was supplied by Cayman Chemical (Ann Arbor, MI, USA) and used as delivered. Lipofectamine® RNAiMax Transfection Reagent is a product of Thermo Fischer Scientific (Waltham, MA, USA). Rabbit anti-NF-κB p105/p50 polyclonal antibody, Alexa Fluor® 488 conjugated, was purchased from Bioss Antibodies (Woburn, MA, USA). Mouse anti-EEA1 antibody was supplied by BD Biosciences (San Diego, CA, USA). Rabbit anti-Rab7 antibody was purchased from Cell Signalling Technology (Danvers, MA, USA). Goat anti-mouse IgG secondary antibody, Alexa Fluor® 647, and goat anti-rabbit IgG secondary antibody, Alexa Fluor® 647, were supplied by Invitrogen (Carlsbad, CA, USA). NFκB Total SimpleStep ELISA™ Kit was purchased from abcam®. HPLC-purified SiRNA against NF-κB were obtained from Sigma-Aldrich (Castle Hill, Australia). HPLC-purified siRNA against luciferase were purchased from Dharmacon, Inc. (Lafayette, CO, USA). Hoechst 33342 and Alexa Fluor® 448 Phalloidin were obtained from Thermo Fisher.

Fluorescence Measurements

Steady-state fluorescence emission spectra of the NF-κB-switch and control sequence were acquired on a Horiba FL-322 Fluorolog-3 spectrophotometer equipped with a 450 W Xenon arc lamp as excitation source. The excitation wavelength, λ_{ex}, was set to 630 nm ($slit_{ex}$ = 10 nm), acquisition window ranged from λ = 650 nm to λ = 720 nm ($slit_{em}$ = 5 nm), and a quartz cuvette of 100 μL in volume was used. All measurements were carried out at 37 °C. Fluorescence emission spectra relevant to the binding curve for NF-κB were obtained by incubating the NF-κB-switch (10 nM) with progressive concentrations of stock NF-κB p50 in the range of 0.1–500 nM. Fluorescence emission spectra of the unwound NF-κB-switch and control sequence were obtained after hybridization with respective complementary oligonucleotides in excess (500 nM).

Cell Culture

Human prostate cancer PC3 cells were cultured in Dulbecco's Modified Eagle Medium (Lonza, Basel, Switzerland) with 4.5 g/L glucose and L-glutamine, supplemented with 10% fetal bovine serum (FBS) and 1% penicillin-streptomycin, at 37 °C and in 5% CO_2. After reaching 80–90% confluency, cells were detached using an enzyme-free dissociation buffer (Gibco, Thermo Fisher) and re-seeded in the relevant culture dish.

DNA Nanoswitch Transfection and Confocal Laser Scanning Microscopy Performed on Fixed Cells

PC3 cells, approximately 50,000, were seeded on a square glass cover slip inside 6-well culture plates, followed by addition of 2 mL culture medium and incubation overnight. Transfection with the NF-κB-switch was then performed using lipofectamine as per the transfection protocol provided by the supplier so that the final concentration of the DNA nanoswitch in each well was 25 nM (2 mL culture medium, 7.5% DNA-lipoplex solution). After incubation for 4 h at 37 °C in 5% CO_2, the transfection medium was discarded and replaced with fresh culture medium, followed by incubation for 24 h. Then, the medium was removed, and the cell layer on the glass cover slip was gently washed with phosphate-buffered saline (PBS, 3×), fixed with 4% paraformaldehyde in PBS (15 min, 25 °C), washed again with PBS (3×), permeabilized with 0.5% Triton X-100 in PBS (5 min, 25°C), blocked with 1% bovine serum albumin in PBS (5 min, 25°C), and rinsed again with PBS. Cell nuclei were stained with Hoechst 33342 (10 min, 25 °C, protected from light) and washed with PBS (3×). The cover slip was then mounted onto a glass slide for microscopy analysis. The same procedure was applied when using the DNA control sequence.

Confocal micrographs were acquired on a Nikon A1R confocal laser scanning microscope. The emission of the NF-κB-switch (Quasar 670) was achieved by exciting at λ = 640 nm and recorded at High Voltage (Gain): 80, Offset: 0, Laser power: 8.0, using the relevant emission filter. The set-up was maintained constant during data acquisition of the control samples. All image processing was carried out with NIS-Elements Confocal (Nikon). For the co-localization experiments, cells were transfected and handled following the aforementioned protocol and stained after fixation with anti-NF-κB p50 antibody, Alexa Fluor 488 (2.5 μg/mL, 1 h, 25 °C). Green emission of the dye-labelled antibody was collected by exciting at λ = 488 nm and using the relevant emission filter.

Sample Preparation and Microscopy Analysis with STORM

Dual-labelled secondary antibodies were prepared as follows: 50 μL secondary antibody AF488 (2 mg/mL in PBS) was mixed with 50 μL of 0.1 M $NaHCO_3$ and 10 μL AF647 (activator dye/reporter dye = 2:1). The reaction proceeded for 30 min at 25 °C in the dark while stirring on a shaking platform. The reaction volume was adjusted to 0.5 mL. Then, the antibody was purified using NAP-5

View Article Online
DOI: 10.1039/C7NR07814E

gel filtration column after equilibration in PBS. PC3 cells, approximately 30,000, were seeded on 8-well Lab-Tek chamber slides, followed by addition of 0.5 mL culture medium and incubation overnight. Transfection with Quasar 570–Quasar 670-labelled NF-κB-switch was achieved using lipofectamine as per the transfection protocol provided by the supplier so that the final concentration of the DNA nanoswitch in each well was 50 nM (0.5 mL culture medium, 30% DNA-lipoplex solution). After incubation for 4 h at 37 °C in 5% CO_2, the transfection medium was discarded. Cell specimens used for early endosome tracking were washed, fixed, permeabilized, and blocked at this stage as reported above, while samples aimed at late endosomes/lysosomes staining were cultured for additional 24 h in fresh culture medium. After cell culture, the cells were fixed and treated as aforementioned. Immunostaining for early endosomes was performed as follows. Cells were incubated with mouse anti-EEA1 primary antibody (2.5 μg/mL, 1 h, 25 °C), washed with PBS (3×), subsequently incubated with Alexa 647/Alexa 488 dual-labelled goat anti-mouse secondary antibody (2 μg/mL, 1 h, 25 °C), and washed again with PBS (3×). Immunostaining for late endosomes and lysosomes was carried out by incubating cells with rabbit anti-Rab7 primary antibody (2.5 μg/mL, 1 h, 25 °C), washing with PBS (3×), then incubating with Alexa 647/Alexa 488 dual-labelled goat anti-rabbit secondary antibody (2 μg/mL, 1 h, 25 °C), and washing again with PBS (3×).

STORM images were acquired using a Nikon N-STORM system configured for total internal reflection fluorescence imaging (TIRF). The perfect focus system and TIRF angle were adjusted and tuned to maximize the signal-to-noise ratio. AF488-, AF555-, and AF647-labelled antibodies and NF-κB-switches tagged with the pair Quasar570–Quasar670 were excited by 488-, 561-, and 647-nm laser lines. No ultraviolet light activation was used. Fluorescence was collected using a Nikon 100× 1.4NA oil immersion objective and passed through a quad-band pass dichroic filter. All time lapses were recorded onto a 256 pixel × 256 pixel region using an EMCCD camera. For each channel, 3000–5000 frames were sequentially acquired. STORM movies were analyzed with the STORM module of the NIS Elements Nikon software.

Real-Time Monitoring of Binding-Induced Fluorescence Switch-On and Live Cell Imaging

PC3 cells, approximately 40,000, were seeded on 12-well culture plates, followed by addition of 1 mL culture medium and incubation overnight. Transfection with the NF-κB-switch was performed using lipofectamine as per the transfection protocol provided by the supplier so that the final concentration of the DNA nanoswitch in each well was 25 nM (1 mL culture medium, 15% DNA-lipoplex solution). After incubation for 4 h at 37°C in 5% CO_2, the transfection medium was discarded and replaced with fresh culture medium. Then, changes in the intracellular fluorescence emission of adherent cells were monitored over time using an Infinite M200 Pro plate reader (Tecan). The excitation wavelength was set to 645 nm, emission wavelength, λ_{em}, was set to 670 nm, and the integration time was set to 20 μs. Fluorescence intensity was recorded at different time points i.e., 0, 4, 8, and 24 h after the initial 4 h-transfection phase. UV-Visible absorption and fluorescence measurements were conducted on an Infinite M200 PRO microplate reader (Tecan Group, Switzerland). A multi-point measurement setting was applied to monitor the fluorescence emission generated in each well (λ_{ex} = 645 nm, λ_{em} = 670 nm).

For the live cell imaging, PC3 cells, approximately 30,000, were seeded on 8-well Lab-Tek chamber slides, followed by addition of 0.5 mL culture medium and incubation overnight. Transfection with the NF-κB-switch was achieved using lipofectamine as per the transfection protocol provided by the supplier so that the final concentration of the DNA nanoswitch in each well was 25 nM (0.5 mL culture medium, 30% DNA-lipoplex solution). After incubation for 4 h at 37 °C in 5% CO_2, the transfection medium was discarded. Nucleus staining was performed with Hoechst 33342 (5 min, under incubation conditions), and fresh culture medium was added to the chamber. Cells were cultured for the next 24 h under usual conditions. Living cells were imaged at different time points while being cultured – 0, 4, 8, and 24 h after completion of the initial transfection phase – using a confocal microscope. The instrumental parameters and emission filters were set as reported above. Control experiments using the control DNA sequence were carried out following the same protocol.

SiRNA-Mediated Knockdown of NF-κB and Flow Cytometry Analysis

The siRNA formulation targeting NF-κB consisted of a 19 basepair duplex with two-nucleotide overhangs on both ends: sense 5′-GGGUAUAGCUUCCCACACU[dT][dT]-3′ and antisense 5′-AGUGUGGGAAGCUAUACCC[dT][dT]-3′. Control siRNA against luciferase (siLuc) consisted of the following sequences: sense 5′-CGUACGCGGAAUACUUCGA[dT][dT]-3′ and antisense 5′-UCGAAGUACUCAGCGUAAGTT[dT][dT]-3′. PC3 cells, approximately 50,000, were seeded in 24-well culture plates, followed by addition of 0.5 mL culture medium and incubation overnight. Transfection with the siRNA formulation was then performed using lipofectamine as per the transfection protocol provided by the supplier so that the final concentration of siRNA in each well was either 50 nM or 200 nM (0.5 mL serum-free medium Opti-MEM, 30% DNA-lipoplex solution). After incubation for 4 h at 37 °C in 5% CO_2, the transfection medium was discarded and replaced with fresh complete culture medium, followed by incubation for the next 24 h. Then, the cells were counter-transfected with the NF-κB-switch following the protocol described above, with a DNA nanoswitch concentration of 25 nM per well (0.5 mL culture medium, 30% DNA-lipoplex solution). After 4 h of incubation, the transfection medium was discarded and replaced with fresh culture medium. The cells were cultured for the next 24 h under usual conditions. Finally, the cells were harvested using enzyme-free cell dissociation buffer, washed with PBS (3×), and immediately analyzed via flow cytometry on an Apogee Flow System. Red 638 fluorescence channel was used to detect intracellular emission of the NF-κB-switch. Data were collected through the dedicated Apogee software and subsequently processed with FlowJo™. All experiments were reproduced in quadruplicate and statistical analysis was carried out using OriginPro (OriginLab™). Abcam's NFκB in vitro SimpleStep ELISA™ (Enzyme-Linked Immunosorbent Assay) kit

View Article Online
DOI: 10.1039/C7NR07814E

was used for the semi-quantitative measurement of NFκB protein in PC3 cells after transfection with 25 nM NF-κB-switch using lipofectamine. PC3 cells, approximately 40,000, were incubated for 4 h at 37°C in 5% CO_2, the transfection medium was discarded and replaced with fresh culture medium. The total concentration of NF-κB of cellular lysates was analysed at different time points i.e., 0, 5, 8, and 22 h after the initial 4 h-transfection, and compared to the supplied control lysate using the plate reader (Tecan).

Results and discussion

A DNA Nanoswitch Targeting the Transcription Factor NF-κB

We set out to use a DNA nanoswitch for the transcription factor NF-κB. The nanoswitch comprises a TF-binding domain (5′-GGGACTTTC-3′ depicted in red circles in Fig. 1a) and interconverts between a non-binding state and a binding-competent state[18] (Fig. 1a and Fig. S1, ESI). The intrinsic equilibrium between a non-binding state ("off-state") and binding-competent state ("on-state") is shifted toward the latter conformation upon interaction with the TF (Fig. 1a). A fluorophore–quencher couple (Quasar 670–Black Hole Quencher BHQ2) conjugated to the sequence (Fig. 1a, b) provides a detectable fluorescence output, indicative of the binding-induced structural motion of the nanoswitch (Fig. 1a).

As the BHQ2 is a contact and a Förster resonance energy transfer quencher, fluorescence emission from the Quasar 670 reporter is only achieved when the two dyes are physically separated via conformational transition that occurs upon TF binding (or because of nuclease hydrolytic activity). NF-κB is a ubiquitous transcription factor mostly studied for its involvement in inflammatory and immune responses, cell proliferation, apoptosis, and cell migration. It has also been reported to play a significant role in cancer development and progression.[21] NF-κB is not a single protein, but rather a complex that naturally binds to the target DNA domain as a homo- or heterodimer depending on the subunits involved. The typical complexes found in the cellular environment are the homodimers p50/p50 and the heterodimers p50/p65, both showing the same DNA-binding domain.[21–23] We initially characterized our NF-κB-switch in terms of binding constant (dissociation constant, K_d) and sensitivity at 37 °C. The NF-κB-switch exhibits a high binding affinity, K_d 66 ± 4 nM, and a fluorescence gain of about 200% at saturating concentrations of NF-κB-p50 (see ESI Section S1, Fig. S2). As a negative control, we designed a non-NF-κB-binding DNA motif (referred to as "control sequence", see Fig. 1b and Fig. S3 see ESI) with the double stem-loop structural features of the NF-κB-switch in the "off-state", however, lacking the TF binding domain.

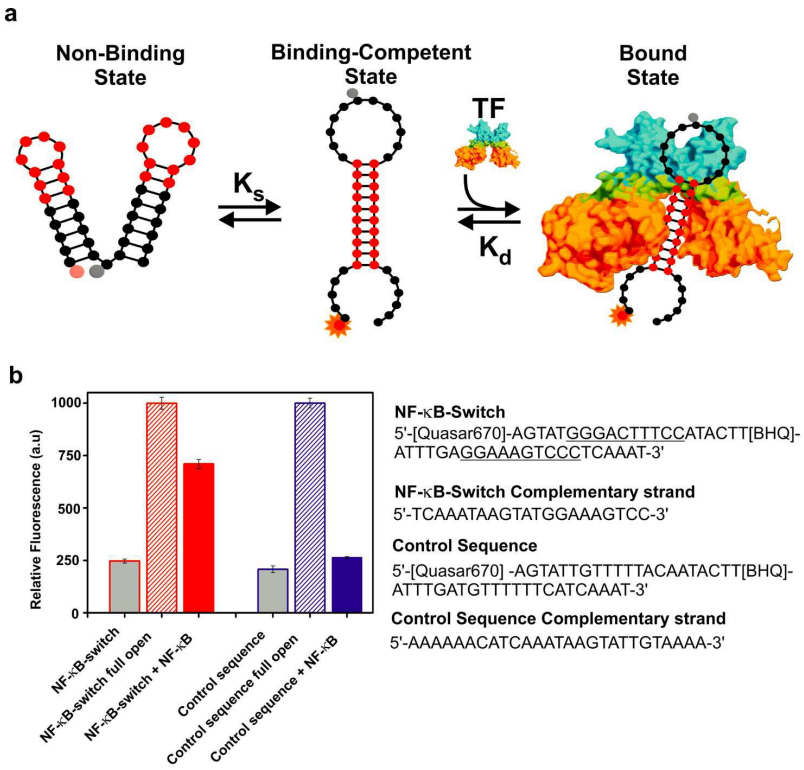

Fig. 1. Binding to NF-κB triggers molecular motion of a DNA nanodevice, allowing intracellular imaging. a) A DNA conformational switch featuring the recognition site for NF-κB (depicted in red circles) is engineered into a molecular switch. b) Fluorescence signal generated from the NF-κB-switch (red) and the control sequence (blue) upon binding to NF-κB or to a DNA complementary sequence. The histogram reports fluorescence intensity values at 37 °C for the NF-κB-switch/control alone, maximum emission for the NF-κB-switch/control unwound upon hybridization with the respective complementary sequences, and fluorescence output for the NF-κB-switch/control incubated with NF-κB. Error

View Article Online
DOI: 10.1039/C7NR07814E

bars refer to standard deviation, *n* = 3. The sequences of the DNA constructs are also shown. In the NF-κB-switch sequence, the underlined segment refers to the domain competent for NF-κB binding.

Although this single conformation control sequence is unable to switch to the "on-state", it ensures a comparable behaviour in terms of nuclease-mediated degradation in the intracellular environment. As confirmed in Fig. S3b (see ESI Section S1), both the NF-κB-switch and the control sequence undergo the same degradation profile when incubated with pure nucleases. Fig. 1b shows a comparative study on the fluorescence output of the NF-κB-switch and the control sequence. Low fluorescence intensity (background fluorescence) is observed for the NF-κB-switch in equilibrium between the two conformations and the double stem-loop control sequence. Equal maximum fluorescence intensity values are obtained when the NF-κB-switch and the control sequence are hybridized with respective complementary sequences that unwind the stem-loop structures into double strands and set the fluorophore and the quencher apart. A large divergence is instead obtained in the presence of target protein NF-κB. In this case, the NF-κB-switch transduces the binding event into a significant fluorescence enhancement. In contrast, the control sequence shows no response. This result is confirmed by comparison of binding curves obtained using the NF-κB-switch and the control sequence (see ESI Section S1, Fig. S2). We note that the fluorescence gain observed when the NF-κB-switch is fully bound to the target protein is slightly lower than that obtained using a complementary DNA strand. This can be ascribed to the fact that the binding-competent state places the reporter fluorophore and the quencher at a distance at which residual quenching is observed. The specificity of the NF-κB-switch for its target was also previously demonstrated.[18] Additionally, gel electrophoresis was employed to confirm formation of the NF-κB/NF-κB-switch complex (Fig. S4, ESI).

Analysis on Fixed Cells after Transfection with the NF-κB-Switch

Based on the above-discussed results, we implemented the present technology for imaging NF-κB binding activity in vitro. We used a prostate cancer PC3 cell line as a test bed. NF-κB is generally kept in an inactive latent state in the cytoplasm of most unstimulated cells, with its activation regulated by the inhibitory IκB proteins through a stimuli-responsive phosphorylation pathway.[21] Conversely, cytoplasmic NF-κB is upregulated and constitutively activated in prostate cancer PC3 cell (i.e., DNA binding activity of NF-κB is constitutively active).[24,25] Cells were transfected for 4 h with NF-κB-switch (25 nM) using Lipofectamine® as a carrier to ensure efficient and reproducible cellular internalization. It is worth noting that naked NF-κB-switch and control sequence are too large and hydrophilic to cross cell membranes.

After the initial incubation, the transfection medium was discarded and the cells were cultured for the following 24 h in fresh culture medium. This was done to avoid overlap of two simultaneous phenomena *i.e.*, binding-induced activation of fluorescence of the NF-κB-switch and uncontrolled enhancement of fluorescence owing to increases in the intracellular concentration of the nanoswitch when delivered to the cells for the whole length of the experiment.

An optimal concentration of NF-κB-switch was used for transfection (25 nM) to ensure signal transduction upon binding to the intracellular TF molecules, taking into account that the NF-κB-switch transfection efficiency is 20%. It is reported that intracellular NF-κB concentration is in the 10-100 nM range in mammalian cells corresponding to approximately ~10^5 copies per cell.[26] In addition, we verified that the transfection of NF-κB-switch does not affect PC3 cell viability (see the MTT assays in ESI Fig. S5). No significant reduction of cell viability was observed after treatment with Lipofecatmine/NF-κB-switch. Firstly, we validated our technique by analysing fixed cells. Confocal laser scanning microscopy (Fig. S6 and Fig. S7, ESI) performed after 24 h incubation revealed a bright red fluorescence emission from the cytoplasm and partially from the nuclei of the cells owing to the nanoswitch binding to NF-κB. No detectable fluorescence signal was generated in the control experiments. This indicated the specific binding-induced nature of the fluorescence signal increase, while also ruling out any artefacts caused by possible degradation of the DNA nanoswitch. The intranuclear fluorescence signal could be ascribed either to a direct diffusion of the NF-κB-switch into the cell nuclei, thus binding to the local fraction of TF, or to the translocation of the NF-κB/DNA-switch complexes after formation in the cytoplasm.

Live Cell Imaging of NF-κB Binding Activity

Thereafter, we assessed the NF-κB-switch as a dynamic probe by performing real-time monitoring of NF-κB binding activity and expression in living cells. After transfection, the fluorescence emission of the NF-κB-switch was monitored over time by recording changes in the signal as binding occurred. Fig. 2 summarizes the results obtained for monitoring populations of live adherent cells in well plates at different time points using a plate reader. We observed a progressive intensification of red emission for the cell samples transfected with the NF-κB-switch.

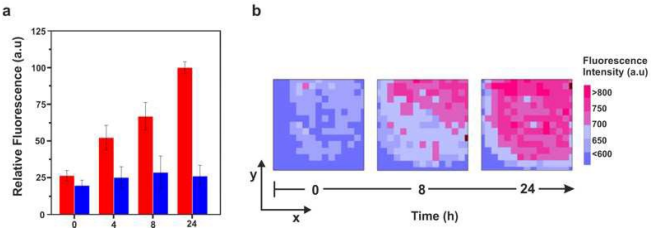

Fig. 2. Real-time imaging of NF-κB binding activity in live cells. a) Histogram showing the fluorescence intensity of populations of living adherent PC3 cells transfected with the DNA nanoswitch, as measured by a plate reader (λex= 645 nm, λem = 670 nm). When the NF-κB-switch is used (red bars), a progressive increase in the fluorescence emission is observed over time, whereas no changes are registered for cells treated with the control sequence (blue bars). Error bars represent standard

View Article Online
DOI: 10.1039/C7NR07814E

deviation, n = 4. b) 2D visual matrices mapping the evolution of the intensity of fluorescence emission in a representative single well containing living adherent PC3 cells over a 24 h after completion of transfection with NF-κB-switch.

The increase in the intensity of the emission over time results from the interconnected dynamics of intracellular trafficking and binding-induced fluorescence emission. Cells transfected with the same amount of control sequence did not show any fluorescence gain (Fig. 2a). The visual matrices in Fig. 2b provide an additional representative mapping of the evolution of fluorescence emission in a single well, showing the progressive increase in total intensity. To confirm this trend, we repeated the same experiment and performed a real-time confocal laser scanning microscopy analysis on living cells (Fig. 3).

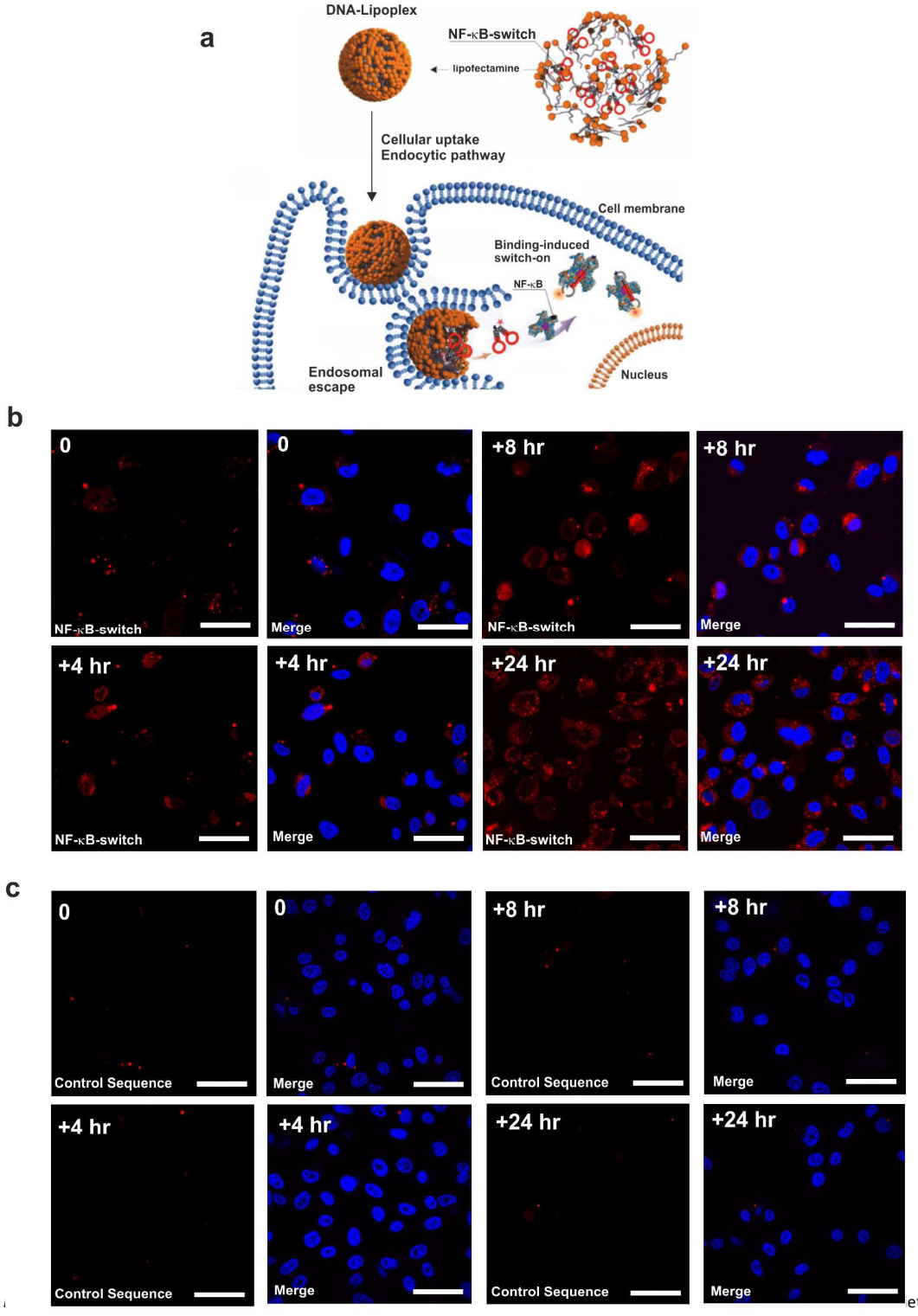

View Article Online
DOI: 10.1039/C7NR07814E

Fig, 3. a) DNA nanoswitches are packaged into DNA-lipoplexes using lipofectamine and internalized into cells via endocytosis. After endosomal escape, the DNA nanodevices are delivered into the cytoplasm and allowed to reach target NF-κB, whose presence is signaled upon binding-induced switch-on of the probes. Confocal micrographs of PC3 cells transfected for 4 h with b) 25 nM of NF-κB-switch or c) the control sequence and imaged at different time points for 24 h, after transfection for 4 h. The cell nuclei are stained in blue with Hoechst 33342. When the NF-κB-switch is used, a bright intracellular red emission can be observed (Quasar 670), which is due to the binding-responsive switching of the DNA probe to the "on-state". Cells treated with the control sequence do not show any intracellular fluorescence emission. Scale bars are 50 μm.

After transfection, cells were imaged at different times within 24 h, thereby allowing for live monitoring of the binding event between the NF-κB-switch and target NF-κB. The confocal panels reported in Fig. 3b show that the time-dependent intracellular fluorescence originated from the binding-induced conformational change of the NF-κB-switch. Control experiments conducted using the control sequence did not show any fluorescence emission over time (Fig. 3c). We also noted fluctuating emission from the cell nuclei, which might be again ascribed to translocation of NF-κB/DNA-switch complexes or dynamic binding of the NF-κB-switch to intranuclear NF-κB. Notably, the above experiments demonstrate that our NF-κB-switch can be effectively used for live cell imaging of NF-κB (activity-based imaging), which is not achievable with standard antibody-based staining techniques that instead require cell fixation and membrane permeabilization.

Specific Binding of the NF-κB-Switch to Its Target

To avoid false positives, it is important to dismiss additional unwanted fluorescence emission triggered by non-specific interactions or degradation. We thus aimed to further confirm the specific binding of the NF-κB-switch to its target inside the cells.

To do so, we co-stained a transfected specimen, after fixation, with a labelled Alexa Fluor® 488 anti-NF-κB p50 antibody (Fig. 4 and Fig. S8 ESI). The standard immunostaining and our DNA-based probing are complementary orthogonal techniques. Confocal micrographs showed nearly perfect co-localization between green (anti-NF-κB p50 antibody staining) and red emission (NF-κB-switch signal), thereby demonstrating the specific recognition and on-target signaling of our NF-κB-switch.

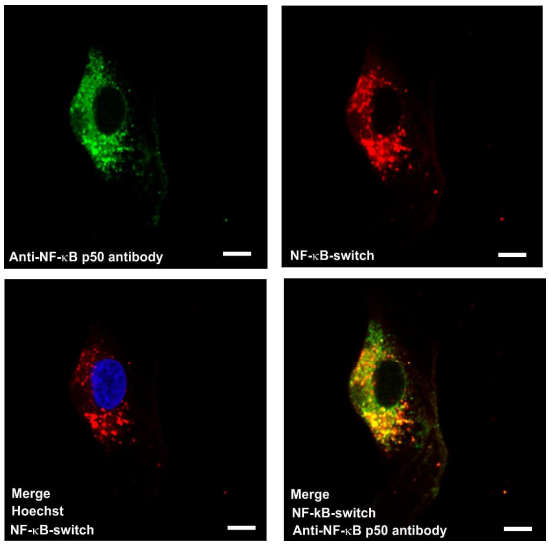

Fig. 4. Confocal micrographs of PC3 cells treated with the NF-κB-switch (25 nM) b) and counter-stained, after fixation, with anti-NF-κB p50 antibody Alexa Fluor 488 labelled a). Co-localization of the green (antibody staining) and red (NF-κB-switch) signals as seen in the merged panel d indicates binding of the DNA nanoswitch to its target transcription factor. Scale bars are 10 μm.

Super-Resolution Microscopy Analysis of Endosomal Escape

To advance the understanding of the cellular route through which the NF-κB-switch reaches and binds to the target, we examined its endocytic trafficking, as depicted in Fig. 3a. Robust proof of substantial endosomal escape, which is often the major bottleneck encountered in the intracellular release of nanoformulations,[27] is important for dismissing that the emission of the NF-κB-switch is not a false positive caused by late lysosomal degradation of entrapped species. We employed stochastic optical reconstruction microscopy(STORM), a super-resolution technique that allows sub-diffraction-limit resolution by reconstructing images on the basis of the accurate localization of single, stochastically blinking emitters.[28,29] We used a NF-κB-switch labelled with Quasar 570–Quasar 670 as an activator–reporter pair, which allows for multi-channel acquisition when different activators are concomitantly used to label target molecules.[30] To track the initial phases of the bio-machinery accounting for the cellular internalization of lipofectamine/NF-κB-switch complexes, we performed immunostaining for early endosomes (anti-EEA1 antibody) and examined the co-localization of these vesicles with the NF-κB-switch. Fig. 5a shows representative STORM micrographs acquired for PC3 specimens after 4 h of incubation. As STORM allows for resolving individual vesicles and nanostructures beyond the diffraction limit of light with 20-nm lateral resolution, compartmentalization (i.e., signal co-localization) of the lipofectamine/NF-κB-switch complexes (red) within early endosomal structures (green) can be investigated. Co-localized early endosomes and lipofectamine/NF-κB-switch complexes were visualized (yellow) down to several tens of nanometer resolution, alongside non-colocalized lipofectamine/NF-κB-switch complexes (Fig. 5a). To demonstrate the effective cytosolic release of the NF-κB-switch, we then aimed at monitoring endosomal escape (Fig. 5b). After transfection (4h), cells were cultured for 24 h, and immunostaining for

View Article Online
DOI: 10.1039/C7NR07814E

Rabankyrin-7 (Rab7) was performed. Rab7 is a marker protein involved in late endosome to lysosome maturation and trafficking, and localized to both the compartments.[31] Notably, this time, we did not observe co- localization between the NF-κB-switch (red) and the vesicles (green), whereas we observed widespread diffusion of the NF-κB- switch in both the cell cytoplasm and the nucleus (Fig. 5b).

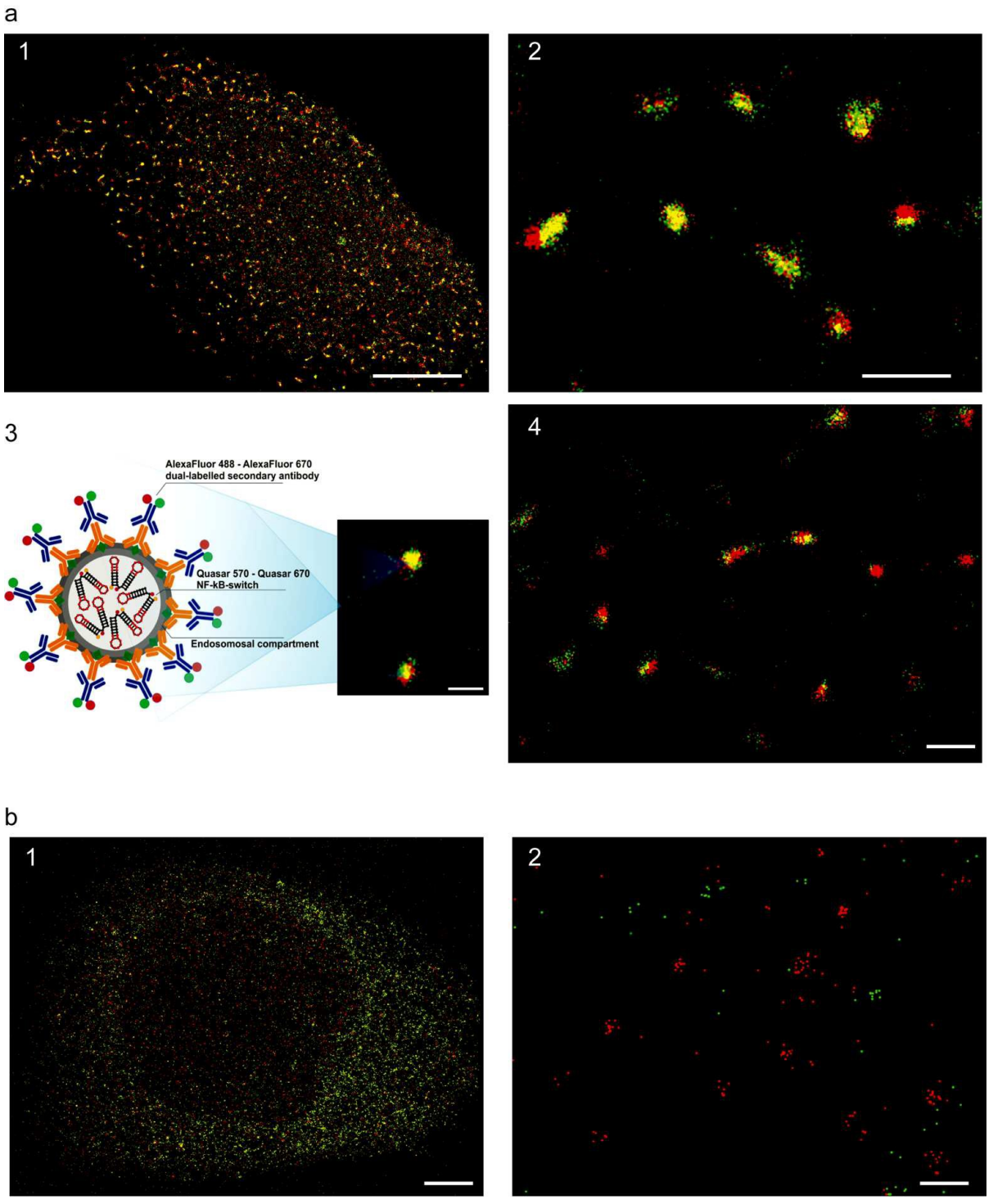

View Article Online
DOI: 10.1039/C7NR07814E

Fig.5. a) Multi-color STORM super-resolution images of the NF-κB-switch and early endosome compartments. Image1: Large view of a PC3 cell featuring early endosome vesicle enclosing NF-κB-switch-lipoplexes. The green signal denotes early endosomes (anti-EEA1 dual-labelled immunostaining), whereas the red signal originates from the NF-κB-switches (pair Quasar570–Quasar670); scale bar is 7 μm. Image 2: Single early endosome/DNA-lipoplex structures at higher magnification, showing both co-localization and endosomal escape; scale bar is 200 nm. Image 3: STORM allows for super-resolved imaging of a single endosomal compartment encapsulating internalized DNA nanoswitches organized in DNA-lipoplexes using lipofectamine as a vehicle. The pictorial scheme shows a representation of the labeling strategy used to perform multi-color imaging of the endocytic pathway, highlighting the activator–reporter pairs used as STORM probes; scale bar is 100 nm. Image 4: A larger view of single early endosome/DNA-lipoplex structures and concurrent escaping objects. Scale bar is 200 nm. b) Multi-color STORM images of the NF-κB-switch and late endosome/lysosome compartments. Image 1: Large view of a PC3 cell featuring non-co-localized late endosomes/lysosomes and NF-κB-switches. The green signal is associated with late endosome/lysosome structures (anti-Rab7 dual-labelled immunostaining), whereas the red signal arises from the NF-κB-switches; scale bar is 3 μm. Images 2: High-magnification image of independent NF-κB-switch aggregates not localized with lysosome compartments; scale bar is 100 nm.

Furthermore, it was possible to spot individual non-co-localized objects at sub-diffraction-limit resolution (Fig. 5b,2). These results clearly indicate rupturing of the vesicles during endosomal escape and subsequent release and diffusion of free NF-κB-switch. To the best of our knowledge, this is the first time the endosomal escape of DNA nanodevices (and nanocomplexes in general) has been monitored and resolved using super-resolution stochastic optical reconstruction microscopy.

A Dynamic Probe for Downstream Quantification of Gene Silencing in living cells

We then assessed whether our NF-κB-switch could be successfully employed as a dynamic probe for monitoring fluctuating NF-κB levels in living cells in response to an applied stimulus. For this purpose, the relative quantification of downstream knockdown of NF-κB expression mediated by siRNA gene silencing is a valid strategy. Cells were first transfected (Fig. 6a) with a siRNA formulation targeting mRNA encoding for NF-κB and, subsequently, with the NF-κB-switch. After 1 day of co-incubation in fresh medium, the living cells were detached and the intracellular fluorescence signal was immediately analysed via flow cytometry (Fig. 6b).

We observed that the final fluorescence emission (i.e. binding-induced switch-on) was finely tuned as an effect of the upstream siRNA knockdown (Fig. 6b,c). Even small variations in NF-κB expression induced by different doses of siRNA treatment[32] could be significantly detected with $p < 0.05$ (Fig. 6b). To further confirm the validity of the siRNA silencing effects, we performed the same experiment and used a labelled anti-NF-κB p50 antibody on fixed cells to stain NF-κB. The results showed a change in NF-κB silencing similar to the one obtained when using the NF-κB-switch (see ESI Fig. S9).

However, we noted that the immunostaining procedure did not produce a significant difference between the two applied siRNA doses, contrary to what we observed when the NF-κB-switch was used. We believe that the latter finer quantification obtained is due to the simplicity and direct use of the NF-κB-switch in live cells. This technology thus allows by-passing all the fixation operations typically needed for antibody staining (*e.g.*, cell permeabilisation, antibody penetration, multiple washing steps) that may lead to a less accurate discrimination. It is also important to point out that the lipofectamine-based delivery of the NF-κB-switch ensures a constant and reproducible transfection, which allows for dismissing inaccurate quantification of NF-κB due to uncontrolled transfection of DNA nanoswitch doses. Transfection with a scramble negative siRNA control did not show a significant variation in the expression of NF-κB, suggesting that the transfection treatment itself does not trigger any signalling response in living cells. This also permits to rule out any unwanted mutual interaction between the siRNA formulation and the DNA nanoswitch inside the cells. Importantly, we also assessed that the total intracellular NF-κB concentration does not undergo any variation because of transfection with NF-κB-switch itself and during its intracellular trafficking (see ESI Fig S10). Our technology allowed for quantifying the magnitude of the siRNA-mediated knockdown of NF-κB, showing as much as 48% and 63% reduction of the fluorescence emission (which is proportional to bio-available NF-κB), respectively, for doses of siRNA of 50 and 200 nM. Notably, this has been achieved by directly analysing populations of living cells, with no need for post-culturing operations or elaborate techniques.

View Article Online
DOI: 10.1039/C7NR07814E

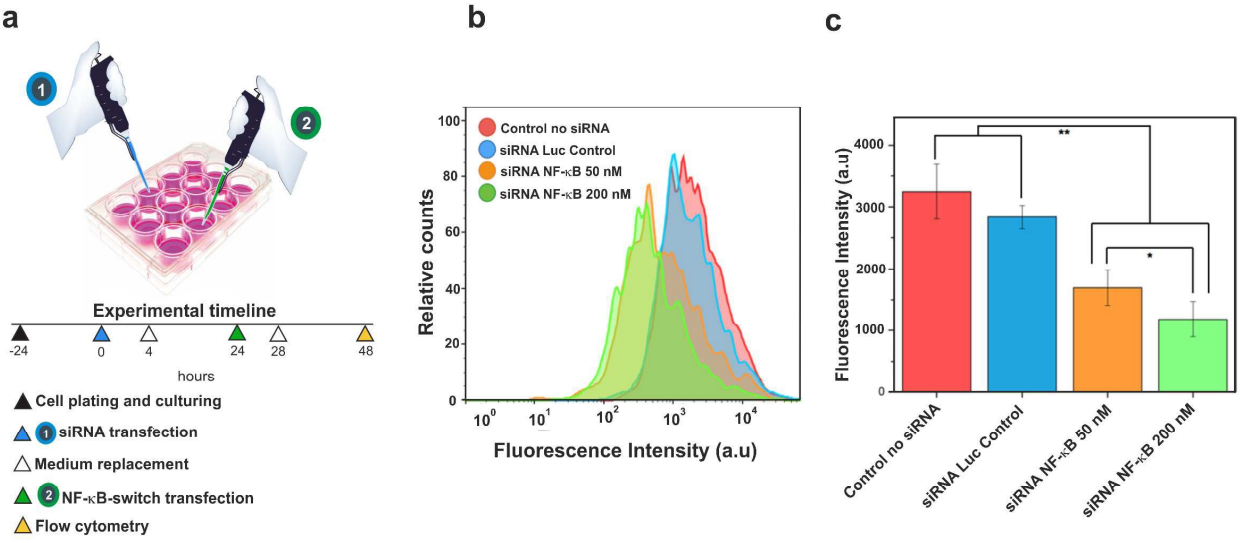

Fig. 6. Real-time downstream monitoring of siRNA-mediated gene silencing. a) Schematic illustration of the experimental timeline followed for co-transfection of cells with siRNA formulations and NF-κB-switch. b) flow cytometry profiles of PC3 cells treated with different siRNA formulations and subsequently transfected with the NF-κB-switch. Representative profiles are reported for cells in the absence of treatment (Control, no siRNA, red line), for cells with an administered 200 nM dose of control siRNA against Luciferase (siRNA Luc Control, blue line), and for cells transfected with doses of respectively 50 nM (siRNA NF-κB 50 nM, orange line) and 200 nm (siRNA NF-κB 200 nM, green line) of siRNA formulation against NF-κB. The fluorescence intensity measured refers to the red emission originating from the binding of the DNA probe to its target NF-κB. c) histogram reporting the mean values of fluorescence intensity collected for the above samples. Experiments are reproduced in quadruplicate, error bars correspond to standard deviations, and statistically significant differences are reported as $* p < 0.05$ and $** p < 0.005$.

Conclusions

We have demonstrated the successful use of a DNA nanoswitch for probing transcription factor binding activity in vitro. Our nanodevice allows for live cell monitoring of a target TF, without resorting to antibody-based staining techniques on fixed cells. Furthermore, the DNA nanoswitch serves as a dynamic probe for sensing and comparatively quantifying in real time the intracellular levels of target TF, with no need for reporter genes. The findings suggest the potential of the nanoswitch as a robust tool for fast and cost-effective screening of siRNA-mediated TF down regulation or, possibly, drug-induced inhibition. The versatility of the DNA scaffold ensures that a vast range of available chemical modifications can be introduced for custom-tuning of the fluorescence properties of the probe. The flexibility of DNA as a functional material also ensures that further engineering of binding-induced molecular motion may be explored to create sophisticated DNA nanodevices with programmable features. Our approach is, in principle, extendable to other families of transcription factors and, more in general, DNA-binding proteins upon design of relevant switching conformations. Given the central role that TFs play in cellular processes, including oncogenic pathways, cell differentiation, and response to environment cues, we believe that our technology may be a powerful tool for molecular biology as it allows for monitoring of intracellular dynamics of TF synthesis, migration, and activation in real time with accurate temporal and spatial resolution.

Conflicts of interest

There are no conflicts of interest to declare.

Acknowledgements

This work was supported by the Australian Research council (ARC) under the Future Fellowship (F.Cav., FT140100873) and Australian Laureate Fellowship (F.Car., FL120100030) schemes. A.B thanks the Australian Government, Department of Education and Training for providing the Endeavour Research Fellowship (#5574) supporting postdoctoral research at The University of Melbourne. This research was also supported by the ARC Centre of Excellence in Convergent Bio-Nano Science and Technology (project number CE140100036) and MSCA-RISE, *NANOSUPREMI* PN: *690901*. This work was performed in part at the Materials Characterisation and Fabrication Platform (MCFP) at The University of Melbourne and the Victorian Node of the Australian National Fabrication Facility (ANFF). We acknowledge Marcin Wojnilowicz and Paul Brannon for assistance with microscopy experiments. We also acknowledge Dr. Jan Fric for helpful discussions.

Notes and references

1 T. Liedl, T. L. Sobey and F. C. Simmel, *Nano Today* 2007, **2**, 36.

View Article Online
DOI: 10.1039/C7NR07814E

2 N. C. Seeman, *Trends Biochem. Sci*. 2005, **30**, 119.
3 J. Bath and A. J. Turberfield, *Nat. Nanotechnol.* 2007, **2**, 275.
4 S. Ranallo, A. Amodio, A. Idili, A. Porchetta and F. Ricci, *Chem. Sci*., 2016, **7**, 66.
5 Y. J. Chen, B. Groves, R. A. Muscat and G. Seelig, *Nat. Nanotechnol*. 2015, **10**, 748.
6 C. Y. Tay, L. Yuan and D. T. Leong, *ACS Nano 2015*, **9**, 5609.
7 S. Surana, A. R. Shenoy and Y. Krishnan, *Nat. Nanotechnol.* 2015, **10**, 741.
8 S. Saha, V. Prakash, S. Halder, K. Chakraborty and Y. Krishnan, *Nat. Nanotechnol.* 2015, **10**, 645.
9 H. Liu and APR Johnston *Angew. Chem*. Int. Ed. 2013, **52**, 5744.
10 J. M. Vaquerizas, S. K. Kummerfeld, S. A. Teichmann and N. M. Luscombe, *Nat. Rev. Genet*. 2009, **10**, 252.
11 G. Badis, M. F. Berger, A. A. Philippakis, S. Talukder, A. R. Gehrke, S. A. Jaeger, E. T. Chan, G. Metzler, A. Vedenko, X. Chen, H. Kuznetsov, C. Wang, D. Coburn, D. E. Newburger, Q. Morris, T. R. Hughes and M. L. Bulyk, *Science* 2009, **324**, 1720.
12 T. Heyduk and E. Heyduk, *Nat. Biotechnol.* 2002, **20**, 171.
13 L. J. Ou, P. Y. Jin, X. Chu, J. H. Jiang and R. Q. Yu, *Anal. Chem*. 2010, **82**, 6015.
14 A. Cao and C. Y. Zhang, *Anal. Chem*. 2013, **85**, 2543.
15 J. J. Liu, X. R. Song, Y. W. Wang, G. N. Chen and H. H. Yang, *Nanoscale* 2012, **4**, 3655.
16 E. A. Smith, M. G. Erickson, A. T. Ulijasz, B. Weisblum and R. M. Corn, *Langmuir* 2003, **19**, 1486.
17 D. L. Ma, T. Xu, D. S. Chan, B. Y. Man, W. F. Fong and C.-H. Leung, *Nucleic Acids Res*. 2011, **39**, e67.
18 A. Vallée-Bélisle, A. J. Bonham, N. O. Reich, F. Ricci and K. W. Plaxco, *J. Am. Chem. Soc*. 2011, **133**, 13836.
19 J. C. M. Gebhardt, D. M. Suter, R. Roy, Z. W. Zhao, A. R. Chapman, S. Basu, T. Maniatis and X. S. Xie, *Nat. Methods* 2013, **10**, 421.
20 H. Carlsen, G. Alexander, L. M. Austenaa, K. Ebihara and R. Blomhoff, *Mutat. Res. Fundam. Mol. Mech. Mutagen* 2004, **551**, 199.
21 M. Karin, Y. Cao, F. R. Greten and Z. W. Li, *Nat. Rev. Cancer* 2002, **2**, 301.
22 F. E. Chen, D. B. Huang, Y. Q. Chen and G. Ghosh, *Nature* 1998, **391**, 410.
23 G. Ghosh, G. Van Duyne, S. Ghosh and P. B. Sigler, P. B. *Nature* 1995, **373**, 303.
24 S. T. Palayoor, M. Y. Youmell, S. K. Calderwood, C. N. Coleman and B. D. Price, *Oncogene* 1999, **18**, 7389.
25 A. V. Gasparian, Y. J. Yao, D. Kowalczyk, L. A. Lyakh, A. Karseladze, T. J. Slaga and I. V. Budunova, *J. Cell Sci.* 2002, **115**, 141.
26 J. Mothes, D. Busse, B. Kofahl and J. Wolf, *BioEssays* 2015, **37**, 452.
27 H. K. Shete, R. H. Prabhu and V. B. Patravale, *J. Nanosci. Nanotechnol*. 2014, **14**, 460.
28 M. J. Rust, M. Bates, X. Zhuang, *Nat. Methods* 2006, **3**, 793.
29 X. Zhuang, *Nat. Photonics* 2009, **3**, 365.
30 M. Bates, B. Huang, G. T. Dempsey and X. Zhuang, *Science* 2007, **317**, 1749.
31 Y. Feng, B. Press and A. Wandinger-Ness, *J. Cell. Biol.* 1995, **131**, 1435.
32 D. W. Bartlett and M. E. Davis, Nucleic Acids Res. 2006, **34**, 322.

View Article Online
DOI: 10.1039/C7NR07814E

TOC

A dynamic DNA nanoswitch is used to probe NF-κB binding activity and its expression level directly in living cells.

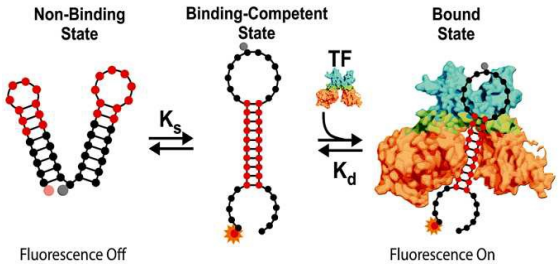

Author/s:
Bertucci, A; Guo, J; Oppmann, N; Glab, A; Ricci, F; Caruso, F; Cavalieri, F

Title:
Probing Transcription Factor Binding Activity and Downstream Gene Silencing in Living Cells with a DNA Nanoswitch

Date:
2018

Citation:
Bertucci, A., Guo, J., Oppmann, N., Glab, A., Ricci, F., Caruso, F. & Cavalieri, F. (2018). Probing Transcription Factor Binding Activity and Downstream Gene Silencing in Living Cells with a DNA Nanoswitch. Nanoscale, 10 (4), pp.2034-2044. https://doi.org/10.1039/C7NR07814E.